

# Human Motion Unlearning

Edoardo De Matteis<sup>1\*</sup> Matteo Migliarini<sup>1,2\*</sup> Alessio Sampieri<sup>2</sup> Indro Spinelli<sup>1</sup> Fabio Galasso<sup>1</sup>  
<sup>1</sup>Sapienza University of Rome, Italy <sup>2</sup>ItalAI

## Abstract

We introduce the task of human motion unlearning to prevent the synthesis of toxic animations while preserving the general text-to-motion generative performance. Unlearning toxic motions is challenging as those can be generated from explicit text prompts and from implicit toxic combinations of safe motions (e.g., “kicking” is “loading and swinging a leg”). We propose the first motion unlearning benchmark by filtering toxic motions from the large and recent text-to-motion datasets of HumanML3D and Motion-X. We propose baselines, by adapting state-of-the-art image unlearning techniques to process spatio-temporal signals. Finally, we propose a novel motion unlearning model based on Latent Code Replacement, which we dub LCR. LCR is training-free and suitable to the discrete latent spaces of state-of-the-art text-to-motion diffusion models. LCR is simple and consistently outperforms baselines qualitatively and quantitatively. Project page: <https://www.pinlab.org/hmu>.

## 1. Introduction

Generative models span across various domains, including images [25, 27], videos [2, 9], and music [6], and in recent years they have achieved remarkable advancements in human motion synthesis [3, 16, 29, 37]. Due to their high performance and impressive generation quality, these models are widely used in applications such as virtual reality [33] and animation [30]. However, undesirable or toxic behaviors are embedded in large training datasets, which raises concerns about safety [35], ethical generation [1], and bias [7]. In fact, models trained on datasets like HumanML3D [14] and Motion-X [19] can generate violent or promiscuous movements, including actions such as *punching*, *kicking*, and other violent movements derived from martial arts.

Machine unlearning has been extensively studied in image generation [11, 12, 20], with approaches ranging from dataset curation [13], which is costly and impractical, to fine-tuning [10, 17, 20], which is computationally demanding and can compromise generation quality. State-of-

\*Equal contribution.

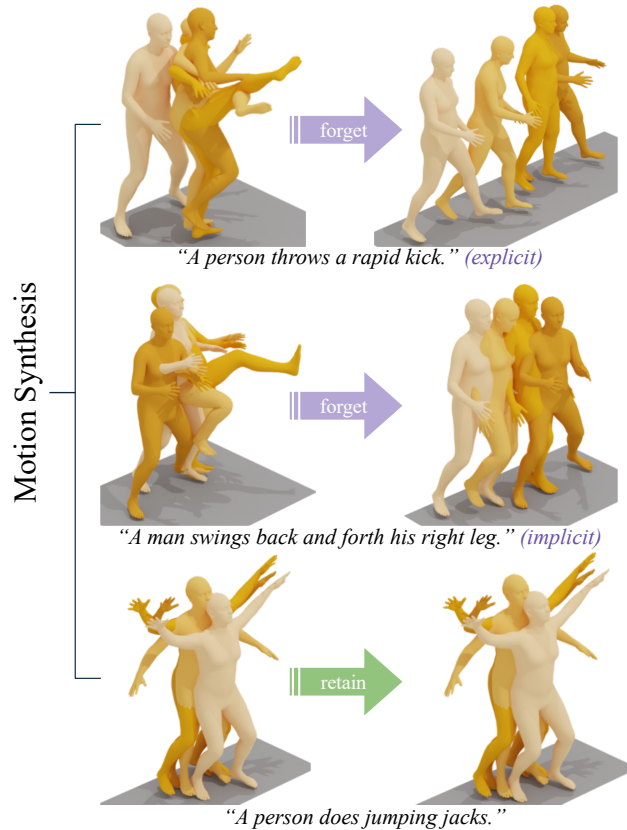


Figure 1. A pictorial illustration of the human motion unlearning process. The methodology takes a textual description as input and generates the corresponding motion if the description is toxic-free. When toxic content is present, the model avoids harmful actions, producing a safe and appropriate outcome.

the-art unlearning techniques now focus on training-free methodologies [11, 12], which remove undesired concepts without modifying datasets or requiring additional training. However, these approaches have been developed primarily for static image generation and do not consider the unique challenges of motion synthesis, such as maintaining temporal consistency across frames and preserving natural dynamics in movement. Moreover, unlearning motions poses an additional challenge: toxic motion can be generated from

explicit text prompts, but also from implicit toxic combinations of otherwise safe motions (e.g., *punching* can emerge from extending an arm after a preparatory retraction).

We propose the first benchmark for unlearning toxicity from large and recent datasets of HumanML3D and Motion-X. We do so by filtering all sequences that contain harmful motions. We propose baselines based on state-of-the-art training-free unlearning techniques from the text-to-image domain, namely UCE [11] and RECE [12], which we extend to human motion synthesis. Specifically, we apply these techniques to leading models in the field, MoMask [15] and BAMB [22], assessing their effectiveness in removing harmful motion patterns while preserving generation quality.

We propose the first motion unlearning technique based on replacing the codebooks of discrete-latent-space, which we dub Latent Code Replacement (**LCR**). Similarly to state-of-the-art image unlearning techniques, LCR is training-free. It specifically suits leading text-to-motion models such as MoMask [15] and BAMB [22], leveraging their use of codebooks. LCR operates directly on the discrete latent space, without modifying the attention mechanisms in transformers [11, 12]. It redirects the generation process away from harmful patterns by modifying the codebook, ensuring that the model produces intended motions without undesirable actions. By interacting solely with the latent space and leaving the model parameters unchanged, LCR minimizes quality degradation while effectively unlearning toxic behaviors.

Our contributions can be summarized as follows:

- *The first human motion unlearning benchmark*: We establish the first benchmark for safe and ethical motion generation, based on HumanML3D and Motion-X, and introduce a filtered version of both datasets without toxic content.
- *Training-Free Unlearning for Motion Synthesis*: We adapt UCE and RECE from text-to-image unlearning to motion models such as MoMask and BAMB, evaluating their effectiveness.
- *Latent Code Replacement*: We propose LCR, a novel unlearning approach that operates directly in the latent space of the codebook, efficiently removing harmful motion patterns. Our method outperforms existing unlearning techniques, setting a new state-of-the-art in human motion unlearning.

## 2. Related Work

The novel task of human motion unlearning relates to machine unlearning and human motion synthesis, both of which have seen significant recent progress. However, they have not been addressed jointly, which is the focus of our proposal.

**Machine Unlearning.** Machine unlearning aims to erase unwanted knowledge from generative models without deteriorating their general performance. It has gained significant attention in generative models, particularly in image synthesis [18, 20, 28], where it is used to remove undesirable concepts without affecting the overall capabilities of the model [35]. The main strategies vary from data removal [4, 13], which retrains models on filtered datasets, to fine-tuning approaches [8, 20], that adjust specific model parameters, and training-free interventions [11, 12], which modify the model’s behavior without additional training. The latter has gained traction due to its efficiency and effectiveness in unlearning targeted concepts while preserving overall model performance.

Current state-of-the-art approaches are the training-free techniques of UCE [11] and RECE [12]. UCE modifies self-attention mechanisms in diffusion models to suppress activations and substitute them with alternative ones. RECE addresses the limitations of UCE by implementing a mechanism that detects and removes unsafe latent embeddings remaining in the latent space, and iteratively unlearns them, ensuring minimal impact on overall generation quality.

Although these techniques have demonstrated strong results in image generation, they have yet to be explored for sequence-based generative tasks like motion synthesis, where structured latent representations and sequential generation raise new challenges. In this work, we bridge this gap by adapting training-free unlearning to human motion synthesis and propose the first benchmark for human motion unlearning.

**Motion Synthesis.** Generating motion given textual descriptions has seen significant advances in recent years [16, 21, 32], driven by the increasing availability of large-scale motion datasets and improvements in deep-generative models. Motion synthesis approaches typically use two main types of representation: continuous [3, 29] or discrete latent representations [5, 15, 37]. State-of-the-art techniques MoMask [15] and BAMB [22] utilize a quantized motion codebook [34], where motion sequences are first encoded into a compact latent space. This discrete representation enables the use of transformer-based models that predict motion tokens, effectively capturing long-term dependencies and improving generation quality.

Despite the maturity of research in motion synthesis, no prior work has addressed motion unlearning, which our work proposes. Our work introduces the first dedicated approach to unlearning in motion synthesis, directly operating on the structured latent space of codebook-based models to remove undesired behaviors while preserving synthesis quality.

### 3. Human Motion Unlearning

Text-to-motion (T2M) models can generate toxic motions that lead to undesirable social effects, due to motion synthesis datasets as HumanML3D [14] and Motion-X [19] containing instances of toxic behaviors, which are problematic when incorporated into generative models. Throughout this work, we use *toxic* as a general term to refer to motions that depict violence, self-harm, or other actions that could be considered unethical or dangerous when synthesized.

**HumanML3D** is a large-scale dataset containing rich motion capture data, which includes human actions such as fights and movements associated with dangerous behaviors like hitting and kicking. In this dataset, 7.7% of the motions contain toxic actions (Figure 2a). The majority of toxic actions focus on combat-related behaviors, such as kicking (3.4%) and punching (1.7%) (Figure 2c). While the remaining 92.3% of motions are considered safe, the presence of these toxic behaviors remains a concern, particularly when generated in inappropriate contexts. Although the proportion of toxic movements is relatively low compared to other datasets, these actions can still pose risks in real-world applications when utilized without adequate safeguards.

**Motion-X** contains a higher proportion of harmful movements than HumanML3D, with 14.9% of its motions classified as toxic (Figure 2b). Motion-X provides data from a variety of real-world and animated scenarios but also includes harmful actions such as kicking (4.9%), the use of weapons (guns, swords), appearing in up to 5% of the dataset, and martial arts techniques like Kung Fu and Taekwondo (Figure 2d). The broader range and higher frequency of toxic behaviors in Motion-X highlight the increased risk of harmful motion synthesis, with the potential for unethical misuse e.g., in violent or aggressive virtual simulations.

Figure 3 provides an example of a surprising fact: even when harmful actions are not explicitly requested, models can still generate toxic content due to implicit prompting. For example, one might say “a man throws a punch” or “a man pulls his arm back and then swings it forward”, and the model could generate a similar motion as a combination of safe movements. This phenomenon has been observed in images by [36]. While harmful features in T2I typically exist in a single static image, T2M involves both spatial and temporal elements, making the task more challenging. Not only do models need to unlearn individual toxic poses (as in images), but they also need to unlearn temporal sequences of poses that may become toxic. A harmful action in motion may not be present in a single pose, but rather emerge from a sequence of movements that build up over time, complicating the process of identifying and unlearning toxic sequences.

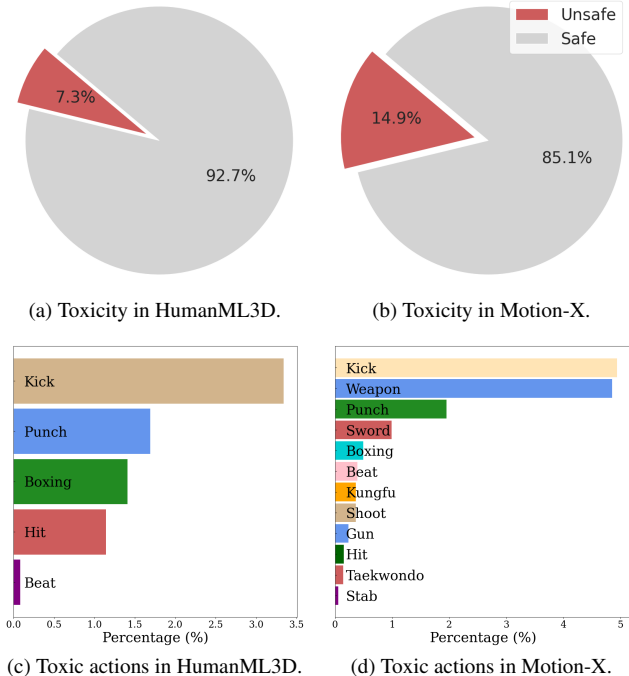


Figure 2. Analysis of toxic actions in HumanML3D and Motion-X. (Top row) Pie charts represent the proportion of toxic actions within each dataset. (Bottom row) Bar plots break down the occurrence of individual toxic actions.

**Problem formalization** Unlearning toxic motions means preventing a model from generating those movements, while preserving its capability to synthesize all other motions. We formalize the problem as follows.

Let us consider the dataset  $\mathcal{D}$  consisting of paired texts  $\mathcal{T}$  and human motions  $\mathcal{M}$ , i.e.  $\mathcal{D} = \{(t, m) \mid t \in \mathcal{T}, m \in \mathcal{M}\}$ . A T2M model parametrized by  $\theta$  is a function  $f_\theta$  able to synthesize novel motions that fall in the same distribution as  $\mathcal{M}$  from textual descriptions.

$$f_\theta(t \sim \mathcal{T}) = m \sim \mathcal{M}. \quad (1)$$

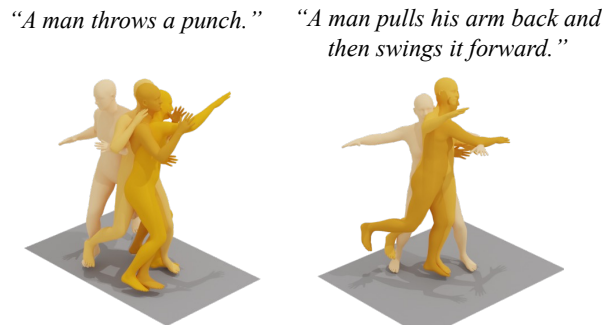


Figure 3. Examples of explicit and implicit toxic actions.

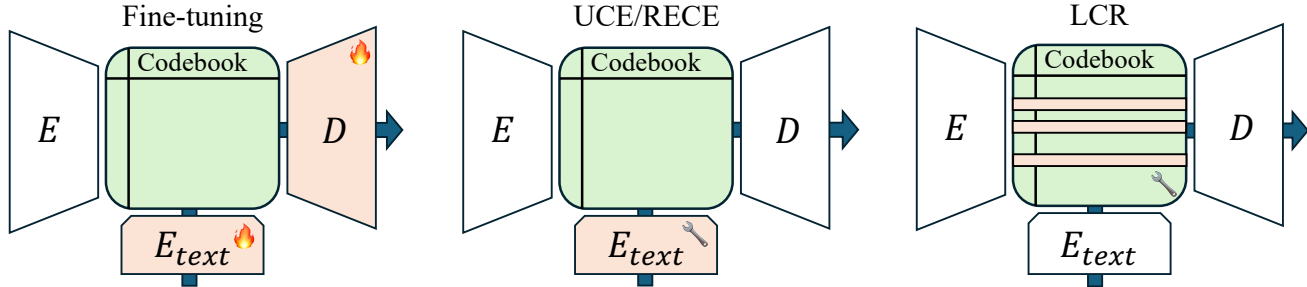


Figure 4. Illustration of motion unlearning approaches: (1) Fine-tuning modifies both the text encoder and motion decoder to remove toxic actions, (2) UCE and RECE, as training-free methods, operate solely on the text encoder, (3) Our proposed LCR selectively updates only the affected codebook entries, ensuring targeted unlearning with minimal impact on overall synthesis quality.

We define a forget set  $\mathcal{D}_f \subseteq \mathcal{D}$  which contains only  $(t, m)$  pairs that we’d like to remove from the model; and accordingly the retain set  $\mathcal{D}_r = \mathcal{D} \setminus \mathcal{D}_f$  of data pairs we consider safe. When unlearning  $\mathcal{D}_f$  from the model  $f_\theta$ , we mean reparametrizing  $\theta \rightarrow \theta'$  such that the model will not be able anymore to generate unsafe motions, while being able to still synthesize motions from the retain dataset’s distribution.

#### 4. Text-to-Motion

We consider the two most recent and best performing text-to-motion models: MoMask [15] and BAMB [22]. Both are based on VQ-VAE [34], encoding auto-regressive motion sequences as latent discrete tokens. And both align text and motion representations. In this section, we review both aspects, specifically referring to MoMask and BAMB.

**Vector Quantized Variational Autoencoders.** VQ-VAE [34] reconstructs the input motion sequence by encoding it into a discrete latent space. Given an input motion sequence  $m \sim \mathcal{M}$ , an encoder  $E(\cdot)$  maps it into a latent representation  $Z \in \mathbb{R}^{T \times d}$  where  $T$  is the length of the motion and  $d$  the dimensionality of latent embedding vector.

Since  $Z$  is continuous, it is discretized to obtain a structured latent representation. This is done by mapping each latent vector  $z_t$  to the closest entry in a learned codebook  $\mathcal{C} = \{c_n\}_{n=1}^N$ , where  $N$  is the number of discrete embeddings. The quantization step is defined as follows:

$$k_t = \arg \min_j \|z_t - c_j\|_2. \quad (2)$$

Thus, each continuous latent vector  $z_t$  is replaced by the nearest codebook entry  $c_{k_t}$  in terms of Euclidean distance. We define  $Z_q(\cdot)$  as the function that maps an input motion sequence  $m$  to its quantized latent representation, i.e.  $Z_q(m) = [k_1, \dots, k_T]$ . The quantized sequence is then passed through a decoder  $D(\cdot)$  to reconstruct the original motion sequence.

The training objective of VQ-VAE consists of three components [15, 16, 37]: **i.** the reconstruction loss ensures that decoded motion sequences remain close to the original input; **ii.** the commitment loss penalizes discrepancies between the encoder output and the selected codebook entries, encouraging stable quantization; **iii.** the codebook update loss adjusts the embeddings to better represent the encoded features, improving discretization over time.

**Aligning text and motion representations.** After learning a motion representation, T2M models align text and motion [3, 15, 22, 29] to ensure semantic consistency between the input text and the generated motion. State-of-the-art models like MoMask [15] achieve this by representing motion as discretized tokens and leveraging transformers to establish alignment with text. At inference, the model generates a sequence of latent indices  $Z \in \mathbb{R}^{T \times d}$  conditioned on a textual prompt  $t$ , using a transformer in an autoregressive manner. Finally, the decoded sequence  $Z$  is passed through the VQ-VAE decoder, trained in the previous stage, to reconstruct the corresponding motion.

#### 5. Modeling Human Motion Unlearning

Here we first extend two state-of-the-art training-free techniques [11, 12] to motion unlearning (Sec. 5.1). Then we introduce our proposed Latent Code Replacement (LCR) model (Sec. 5.2).

##### 5.1. From Image to Motion Unlearning

We redefine UCE [11] and RECE [12] in the context of forgetting motions.

**UCE** enables fast and efficient unlearning for text-to-image models without requiring fine-tuning, modifying the cross-attention between text embeddings and latent image samples. Similarly to UCE, we retain the text embedding but instead of working with images, we use motion embeddings  $Z$ , obtained from the VQ-VAE encoder. Additionally,

unlike text-to-image (T2I) models, we do not modify the cross-attention layers. Given a forget set  $F$  containing text embeddings  $e_f$  associated with toxic concepts (e.g., “punch someone”), UCE modifies the key/value projection matrix  $W_{k/v}$  to align these embeddings with a safe target concept  $\bar{e}_r$  chosen a priori e.g., the empty string. At the same time, it preserves a set of retained concepts  $R$ . The problem is formalized as follows:

$$\begin{aligned} \min_{W^{new}} \sum_{e_f \in F} \|W^{new} e_f - W^{old} \bar{e}_r\|_2^2 \\ + \lambda_1 \sum_{e_r \in R} \|W^{new} e_r - W^{old} e_r\|_2^2 \\ + \lambda_2 \|W^{new} - W^{old}\|_F^2. \end{aligned} \quad (3)$$

Here,  $\lambda_1$  and  $\lambda_2$  are hyperparameters that control the extent to which retained concepts are preserved. As shown in [11], a closed-form solution exists for Eq. 3. We follow the same objective of removing toxic concepts while preserving safe ones. However, state-of-the-art T2M models [5, 15, 16, 22, 37] are codebook-based and handle text conditioning differently from T2I models. Whereas T2I models typically use cross-attention for this purpose [23, 26], most T2M architectures inject text-conditioning by concatenating a textual embedding with the motion latent. To adapt UCE to this setting, we modify the projection matrix  $W$  that maps text embeddings to the motion latent space. Specifically, we apply UCE at the layer between the text encoder [24] and the first self-attention layer, where text and motion embeddings are concatenated. As we show in Sec. 6.1, this effectively steers the model away from toxic generation while maintaining strong performance on the retain set. UCE maps a toxic concept  $e_f$  to the target  $\bar{e}_r$ ; however, it generates toxic content when selecting embeddings that are in close proximity to a forgotten concept.

**RECE** builds upon UCE to completely eliminate the presence of  $F$ ’s embeddings in the latent space  $E$  [12].

RECE looks for the closest textual embedding  $e'_f$  to an unlearned target concept  $e_f$ , then applies UCE to map  $e'_f$  to the safe target  $\bar{e}_r$ . This process is repeated for a pre-defined number of iterations, remapping neighboring toxic concepts to a safe prompt. We adapt this approach to motion: we identify the closest motion embeddings to toxic ones and modify  $W$  to ensure that unsafe textual embeddings are mapped to safe motions using UCE.

## 5.2. Latent Code Replacement

Our proposed Latent Code Replacement unlearning model is based on the key intuition that each code in the VQ-VAE’s codebook encodes a specific motion, and that it is possible to identify toxic codes and replace them with safe

ones. Unlike previous methodologies that modify attention parameters [11, 12, 20], **LCR** intervenes in the codebook’s discrete latent space, enabling more precise control at the representational level under two basic assumptions: **i.** motion codes represent disentangled actions; **ii.** toxic motions can be identified.

The former follows from the theory of VQ-VAE, where codebook discretization inherently encourages concept disentanglement [31]. This is further supported by empirical evidence: removing the codebooks associated with toxic motion does not degrade the generative performance, either quantitatively or qualitatively (cf. Sec. 6.1). Interestingly, the same codebooks can inject toxic behaviors, compromising safe actions, as demonstrated in Sec. 3 of the supplementary materials.

This targeted intervention results in less disruption to the overall generation process while effectively removing toxic patterns. By preserving the integrity of the learned parameters and selectively altering problematic codes in the latent space, our approach maintains generation quality for non-toxic motions while successfully eliminating undesirable behaviors.

**Detecting and Replacing Toxic Motion Codes.** Given a trained codebook  $\mathcal{C}$ , we first identify the set of “forget codes”  $\mathcal{C}_f$  that strongly correlate with undesirable motions:

$$\mathcal{C}_f = \{c \in \mathcal{C} \mid c \propto \mathcal{D}_f\}, \quad (4)$$

where  $c \propto \mathcal{D}_f$  indicates correlation between code  $c$  and samples in the forget set  $\mathcal{D}_f$ . We quantify this correlation by calculating the forget-to-retain ratio for each code. Specifically, for each code  $k$ , we compute:

$$N_k(\mathcal{D}) = \sum_{m \in \mathcal{D}} \mathbb{1}\{k \in Z_q(m)\} \quad (5)$$

$$s_k = \frac{N_k(\mathcal{D}_f)}{N_k(\mathcal{D}_r)}. \quad (6)$$

Where  $N_k(\mathcal{D})$  counts the occurrences of code  $k$  in dataset  $\mathcal{D}$ , and  $Z_q(m)$  represents the set of codes activated by motion  $m$ . As a decision criteria we select the top- $r$  codes with highest  $s_k$  values to form  $\mathcal{C}_f$ , identifying codes that frequently appear in toxic motions but rarely in safe ones.

Our unlearning approach, formalized in Algorithm 1, operates directly on the discrete latent space without modifying model parameters. First, we compute a toxicity score  $s_k$  for each code by measuring its relative frequency in toxic versus safe motions. We then identify the top- $r$  codes with the highest toxicity scores, which represent the discrete tokens most strongly associated with undesirable movements. Once these toxic codes are identified, we replace each one with a randomly sampled safe code  $\bar{c}$  from the complement

	Forget Set				Retain Set			
	FID $\rightarrow$	MM-Notox $\downarrow$	Diversity $\rightarrow$	R@1 $\rightarrow$	FID $\downarrow$	MM-Notox $\downarrow$	Diversity $\rightarrow$	R@1 $\uparrow$
MoMask $\mathcal{D}_r$	13.644 $\pm$ .365	4.392 $\pm$ .041	7.611 $\pm$ .088	0.129 $\pm$ .004	0.093 $\pm$ .003	2.700 $\pm$ .007	10.059 $\pm$ .080	0.291 $\pm$ .001
MoMask [15]	0.956 $\pm$ .084	5.047 $\pm$ .031	6.146 $\pm$ .092	0.159 $\pm$ .005	0.064 $\pm$ .002	2.714 $\pm$ .005	10.143 $\pm$ .081	0.290 $\pm$ .001
MoMask $FT$	1.589 $\pm$ .116	4.912 $\pm$ .033	6.439 $\pm$ .088	0.148 $\pm$ .006	0.088 $\pm$ .002	2.803 $\pm$ .007	10.143 $\pm$ .097	0.280 $\pm$ .001
MoMask w/ UCE	25.039 $\pm$ .442	5.106 $\pm$ .045	8.693 $\pm$ .067	0.105 $\pm$ .005	0.395 $\pm$ .008	3.101 $\pm$ .007	10.194 $\pm$ .091	0.257 $\pm$ .001
MoMask w/ RECE	58.487 $\pm$ .899	8.183 $\pm$ .047	8.591 $\pm$ .073	0.069 $\pm$ .004	12.557 $\pm$ .092	6.531 $\pm$ .015	9.612 $\pm$ .147	0.121 $\pm$ .001
MoMask w/ LCR	<b>12.434</b> $\pm$ .303	<b>4.723</b> $\pm$ .035	<b>6.580</b> $\pm$ .066	<b>0.133</b> $\pm$ .004	<b>0.077</b> $\pm$ .002	<b>2.720</b> $\pm$ .005	<b>10.106</b> $\pm$ .086	<b>0.287</b> $\pm$ .001
BAMM $\mathcal{D}_r$	15.604 $\pm$ .334	4.552 $\pm$ .041	7.688 $\pm$ .074	0.122 $\pm$ .005	0.566 $\pm$ .015	3.123 $\pm$ .009	10.092 $\pm$ .093	0.279 $\pm$ .001
BAMM [22]	1.353 $\pm$ .107	4.911 $\pm$ .053	6.202 $\pm$ .089	0.164 $\pm$ .007	0.135 $\pm$ .004	2.698 $\pm$ .009	10.118 $\pm$ .100	0.302 $\pm$ .001
BAMM $FT$	1.443 $\pm$ .118	4.914 $\pm$ .050	6.224 $\pm$ .098	0.161 $\pm$ .006	0.163 $\pm$ .005	2.731 $\pm$ .007	10.109 $\pm$ .086	0.301 $\pm$ .002
BAMM w/ UCE	57.953 $\pm$ .893	7.809 $\pm$ .068	9.482 $\pm$ .073	0.074 $\pm$ .003	4.296 $\pm$ .063	5.119 $\pm$ .014	9.654 $\pm$ .080	0.184 $\pm$ .001
BAMM w/ RECE	34.367 $\pm$ .484	6.796 $\pm$ .048	<b>7.740</b> $\pm$ .073	0.061 $\pm$ .004	13.310 $\pm$ .118	7.062 $\pm$ .015	8.470 $\pm$ .094	0.122 $\pm$ .001
BAMM w/ LCR	<b>9.712</b> $\pm$ .214	<b>4.597</b> $\pm$ .033	6.502 $\pm$ .077	<b>0.136</b> $\pm$ .005	<b>0.140</b> $\pm$ .005	<b>2.699</b> $\pm$ .008	<b>10.068</b> $\pm$ .102	<b>0.299</b> $\pm$ .001

Table 1. Results on HumanML3D dataset. Method  $\mathcal{D}_r$  reports performances for the model trained on a toxicity-free dataset. Method presents the plain model’s performance, while Method  $FT$  shows the results of fine-tuning the model on the toxicity-free dataset. Then we compare training-free unlearning methodologies.

set  $\mathcal{C} \setminus \mathcal{C}_f$ , plus a small noise term  $\varepsilon$ . This noise term ensures uniqueness among the replacements, preventing potential collisions that could affect the model’s generation diversity. When the autoregressive model subsequently attempts to generate toxic movements, these modified codes redirect the generation toward safe motions instead.

## 6. Benchmark

In this section, we first introduce the datasets and evaluation metrics adapted for motion unlearning. We then compare our proposed LCR method against existing approaches, demonstrating its effectiveness in removing toxic actions while preserving motion quality.

**Datasets.** Starting from two large-scale text-to-motion datasets, HumanML3D [14] and Motion-X [19], we define

---

### Algorithm 1 Latent Code Replacement (LCR)

---

**Require:** Trained codebook  $\mathcal{C}$ , forget dataset  $\mathcal{D}_f$ , retain dataset  $\mathcal{D}_r$ , number of codes to replace  $r$ .

**Ensure:** Modified codebook with unlearned toxic concepts

```

1: codeFrequency  $\leftarrow \emptyset$ 
2: for each code  $k$  in codebook  $\mathcal{C}$  do
3:    $N_k(\mathcal{D}_f) \leftarrow \sum_{m \in \mathcal{D}_f} \mathbb{1}\{k \in Z_q(m)\}$ 
4:    $N_k(\mathcal{D}_r) \leftarrow \sum_{m \in \mathcal{D}_r} \mathbb{1}\{k \in Z_q(m)\}$ 
5:    $s_k \leftarrow \frac{N_k(\mathcal{D}_f)}{N_k(\mathcal{D}_r)}$ 
6:   codeFrequency[ $k$ ]  $\leftarrow s_k$ 
7: end for
8:  $\mathcal{C}_f \leftarrow \text{TopK}(\text{codeFrequency}, r)$ 
9:  $\bar{c} \leftarrow \text{sample}(\mathcal{C} \setminus \mathcal{C}_f)$ 
10: for each code  $c_f$  in  $\mathcal{C}_f$  do
11:    $c_f \leftarrow \bar{c} + \varepsilon$ 
12: end for
13: return  $\mathcal{C}$ 

```

---

the Forget set  $\mathcal{D}_f$  by filtering selected toxic actions from the whole dataset  $\mathcal{D}$ , and the Retain set  $\mathcal{D}_r = \mathcal{D} \setminus \mathcal{D}_f$  as the complementary of  $\mathcal{D}_f$ .

HumanML3D is one of the most widely used benchmarks in T2M research, containing 14.6k human motion sequences with 44.9k detailed textual descriptions. Motion-X provides 81k motion-text pairs.

This filtering process relies on a predefined set of toxic keywords,  $w$ , which we curate manually and have already presented in Figures 2c and 2d. A text-motion pair  $(t, m)$  is assigned to  $\mathcal{D}_f$  if at least one keyword  $w_i$  appears in any prompt within  $\mathcal{T}$ . Conversely, pairs are included in  $\mathcal{D}_r$  only if none of the keywords appears in the prompt.

**Baselines.** We evaluate motion unlearning using MoMask [15] and BAMM [22], two state-of-the-art T2M models. MoMask employs a motion masking strategy within a VQ-VAE framework, while BAMM uses a bidirectional masked transformer for improved text-motion alignment. We extend both models with UCE [11] and RECE [12] to assess their unlearning effectiveness as defined in Sec. 5.1. To establish an upper bound for performance, we retrained both models on a dataset from which all toxic actions were removed ( $\mathcal{D}_r$ ). This allows us to assess the best achievable results when no harmful data are present, serving as a reference point for evaluating the impact of unlearning methods. In each table, the first row (Method  $\mathcal{D}_r$ ) shows the results of the methodology trained on a dataset without toxicity. The second row (Method) shows the results of the plain model, while Method  $FT$  defines the outcomes of the model fine-tuned on the toxicity-free dataset.

**Metrics.** We adapt T2M evaluation metrics to assess unlearning effectiveness. It is expected that the upper bound (Method  $\mathcal{D}_r$ ) underperforms on  $\mathcal{D}_f$ , since we are testing it on a set of toxic actions which it never saw, but we also expect this performance not to drop too abruptly, since T2M

	Forget Set				Retain Set			
	FID $\rightarrow$	MM-Notox $\downarrow$	Diversity $\rightarrow$	R@1 $\rightarrow$	FID $\downarrow$	MM-Notox $\downarrow$	Diversity $\rightarrow$	R@1 $\uparrow$
MoMask $\mathcal{D}_r$	8.435 $\pm$ .295	11.254 $\pm$ .064	15.721 $\pm$ .255	0.119 $\pm$ .007	4.508 $\pm$ .103	8.270 $\pm$ .015	19.560 $\pm$ .332	0.332 $\pm$ .002
MoMask [15]	2.028 $\pm$ .127	9.001 $\pm$ .071	15.884 $\pm$ .219	0.289 $\pm$ .008	2.686 $\pm$ .045	8.076 $\pm$ .017	19.366 $\pm$ .214	0.344 $\pm$ .001
MoMask <i>FT</i>	2.072 $\pm$ .099	9.085 $\pm$ .050	15.855 $\pm$ .050	0.280 $\pm$ .007	3.325 $\pm$ .060	8.070 $\pm$ .019	19.405 $\pm$ .228	0.347 $\pm$ .002
MoMask w/ UCE	<b>10.522</b> $\pm$ .223	10.931 $\pm$ .028	6.648 $\pm$ .112	<b>0.033</b> $\pm$ .001	3.740 $\pm$ .041	6.863 $\pm$ .008	6.243 $\pm$ .059	0.046 $\pm$ .001
MoMask w/ RECE	12.704 $\pm$ .327	12.422 $\pm$ .034	6.241 $\pm$ .132	0.031 $\pm$ .003	14.287 $\pm$ .133	7.351 $\pm$ .013	6.342 $\pm$ .062	0.029 $\pm$ .001
MoMask w/ LCR	2.218 $\pm$ .159	<b>9.930</b> $\pm$ .092	<b>15.606</b> $\pm$ .210	0.283 $\pm$ .007	<b>2.656</b> $\pm$ .043	<b>8.261</b> $\pm$ .019	<b>19.260</b> $\pm$ .216	<b>0.335</b> $\pm$ .001

Table 2. Results on Motion-X dataset.

models are capable of some zero-shot generalization. The unlearned models should mimic the upper bound Method  $\mathcal{D}_r$  as closely as possible. On  $\mathcal{D}_r$ , the interpretations align with standard T2M [15, 16, 22, 29, 37], as the model aims to generate the best possible motions given the textual descriptions.

FID measures the distributional gap between generated and real motions, R-Precision evaluates text-motion relevance, and Diversity captures motion variability.

We additionally introduce MM-Notox, an adaptation of the standard Multi-modal distance (MM-Dist), to measure the distance between text and motion embeddings in unlearning scenarios. For the forget set, MM-Notox computes the alignment between de-toxified generated motions and text where all toxic words have been removed. In the retain set, MM-Notox and MM-Dist yield the same performance, as there is no modification to the textual descriptions. This ensures a fair assessment of how well the model generates non-toxic motions while preserving its synthesis capabilities.

## 6.1. Comparison

In this section, we present the human motion unlearning performances.

**HumanML3D.** Table 1 (top) highlights the performance of MoMask combined with the LCR unlearning method. In the Forget Set, MoMask w/ LCR achieves the best FID, R@1 and Diversity, indicating a generated movement similar to MoMask  $\mathcal{D}_r$  and demonstrating LCR’s ability to reduce toxicity without compromising output variety. In the Retain Set, LCR maintains a strong MM-Notox score, improving MoMask w/ UCE by 7.2%.

In Table 1 (bottom), BAMB w/ LCR strikes the best balance between motion quality and toxicity removal in the forget set, maintaining an FID of 9.712 and achieving an MM-Notox of 4.597, outperforming RECE (+47.8%) and UCE (+69.8%). For the retain set, LCR maintains an FID of 0.140, closely matching BAMB (0.135, -3.7%), and shows superior matching and retrieval scores compared to RECE and UCE, ensuring better retention of non-forgotten data.

**Motion-X.** Table 2 shows the performance of the methodology on the Motion-X dataset. In the forget set, LCR achieves the best diversity, as well as a MM-Notox score that is 9.1% lower compared to the second-best technique. In the Retain Set, LCR outperforms all other methods across every metric, improving the R@1 by 29.1% while maintaining an FID comparable to that of the original MoMask [15]. Results of motion unlearning from BAMB on Motion-X are in Sec. 2 of the supplementary material.

## 7. Discussion

In this section, we first present ablation studies that evaluate the impact of different factors, such as the number of codebooks to be replaced and how unlearning specific actions affects the proposed methodology. Then, we provide qualitative results by comparing generated images from our method to those produced by other techniques.

**Varying the Number of Replaced Codebooks.** Table 3 examines the impact of replacing different numbers of codebooks in LCR. Replacing 4 codebooks (LCR 4) improves the forget set, lowering FID compared to MoMask  $\mathcal{D}_r$ . However, excessively low FID suggests the persistence of toxic movements, whereas MoMask  $\mathcal{D}_r$ ’s high FID reflects its failure to generate them. Increasing replacements to 8 and 16 (LCR 8, LCR 16) reduces the FID gap and lowers MM-Notox, indicating better synthesis of non-toxic movements. Beyond 16 (LCR 32), performance declines. The retain set remains stable, confirming that there is no impact on safe actions.

**Action removing.** Tables 4 and 5 analyze the impact of removing specific toxic actions. We target the most common: *kick* (3.4% in HumanML3D, 4.9% in Motion-X), and the least frequent (*beat* in HumanML3D, *stab* in Motion-X, both less than 0.2%).

Removing *kick* increases FID scores, suggesting reduced toxicity while maintaining description consistency, as MM-Notox remains stable. Also, removing *beat* in HumanML3D is effective (high FID, low MM-Notox), whereas *stab* in Motion-X proves harder to remove (low FID, low MM-Notox).

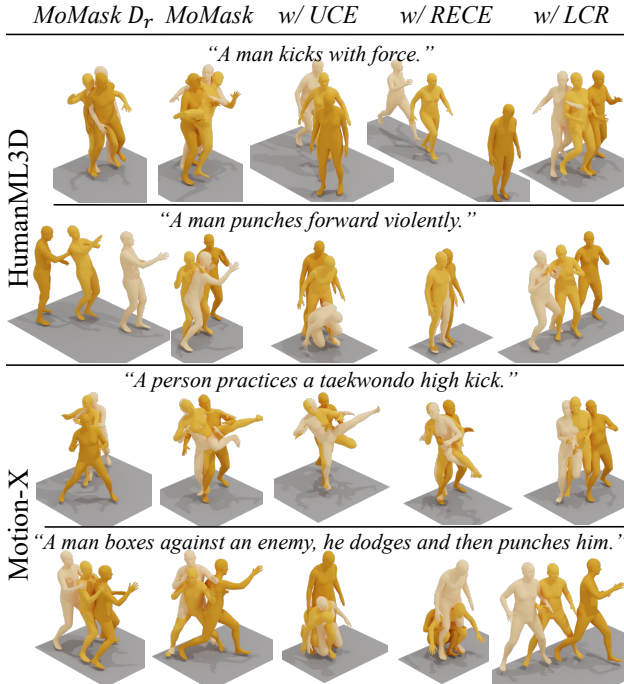


Figure 5. Qualitative comparison of generated motions across datasets. The first two rows present motion samples from HumanML3D, while the last two rows depict samples from Motion-X, illustrating the effectiveness of the proposed unlearning approach. Please see the supplementary video.

	Forget Set			
	FID $\rightarrow$	MM-Notox $\downarrow$	Diversity $\rightarrow$	R@1 $\rightarrow$
MoMask $\mathcal{D}_r$	13.644	4.392	7.611	0.129
MoMask w/ LCR 4	3.567	4.759	6.508	0.142
MoMask w/ LCR 8	10.946	4.744	<b>6.615</b>	0.135
MoMask w/ LCR 16	<b>12.863</b>	<b>4.739</b>	6.569	0.135
MoMask w/ LCR 32	15.304	4.836	6.483	<b>0.129</b>
	Retain Set			
	FID $\downarrow$	MM-Notox $\downarrow$	Diversity $\rightarrow$	R@1 $\uparrow$
MoMask $\mathcal{D}_r$	0.093	2.702	10.059	0.291
MoMask w/ LCR 4	<b>0.066</b>	<b>2.707</b>	10.131	<b>0.290</b>
MoMask w/ LCR 8	0.073	2.714	10.112	0.287
MoMask w/ LCR 16	0.078	2.721	<b>10.107</b>	0.287
MoMask w/ LCR 32	0.081	2.745	9.997	0.285

Table 3. Ablation on number of codebook entries replaced on HumanML3D.

The forget set highlights how the impact varies by action, while the retain set confirms that safe actions remain unaffected, with performance aligning with the baseline.

**Qualitative results.** Figure 5 shows a qualitative comparison between the proposed method (LCR) and UCE and RECE. In HumanML3D, it is evident that the movements generated by LCR are similar to those of MoMask  $\mathcal{D}_r$ , where no toxicity is present. For the actions in Motion-X, it is noticeable that UCE and RECE either hint at toxic actions

		Forget Set			
		FID	MM-Notox	Diversity	R@1
MoMask w/ LCR	<i>all</i>	12.863	4.739	6.569	0.135
	<i>kick</i>	18.652	4.868	5.087	0.077
	<i>beat</i>	20.531	4.935	5.035	0.076
		Retain Set			
		FID	MM-Notox	Diversity	R@1
MoMask w/ LCR	<i>all</i>	0.078	2.721	10.107	0.287
	<i>kick</i>	0.071	2.756	10.101	0.287
	<i>beat</i>	0.069	2.759	10.102	0.290

Table 4. Single concept unlearning on HumanML3D.

		Forget Set			
		FID	MM-Notox	Diversity	R@1
MoMask w/ LCR	<i>all</i>	2.218	9.930	15.606	0.283
	<i>kick</i>	13.163	9.935	15.573	0.163
	<i>stab</i>	1.103	7.098	5.401	0.035
		Retain Set			
		FID	MM-Notox	Diversity	R@1
MoMask w/ LCR	<i>all</i>	2.656	8.261	19.260	0.335
	<i>kick</i>	2.973	8.311	19.071	0.333
	<i>stab</i>	2.613	8.378	19.314	0.334

Table 5. Single concept unlearning on Motion-X.

or remain stationary without performing any actions, while LCR preserves the overall motion without introducing undesirable movements.

**Limitations.** We envision that motion unlearning may be subject to misuse, for example forgetting safe actions to some degree could implicitly emphasize toxic ones. The original UCE and RECE, their motion unlearning extensions, and the proposed LCR may be prone to such misuse.

## 8. Conclusions

Text-to-motion (T2M) synthesis models are essential for character animation in 3D animation and AR/VR applications. Ensuring their safety and ethical integrity requires addressing toxic behaviors in motion generation. In this work, we introduce the novel task of human motion unlearning and establish the first benchmark for this challenge. We propose a training-free method that effectively removes toxic motions while preserving generation quality. Our approach represents the first spatio-temporal framework for motion unlearning, laying the foundation for future advancements in video unlearning. By addressing these challenges, we contribute to developing safer and more reliable motion synthesis models.

**Acknowledgements** We thank Luca Franco for the valuable insights and discussions. We acknowledge support from Panasonic, the PNRR MUR project PE0000013-FAIR, and HPC resources provided by CINECA.

## References

- [1] Hritik Bansal, Da Yin, Masoud Monajatipoor, and Kai-Wei Chang. How well can text-to-image generative models understand ethical natural language interventions? In *EMNLP (Short)*, 2022. 1
- [2] Andreas Blattmann, Robin Rombach, Huan Ling, Tim Dockhorn, Seung Wook Kim, Sanja Fidler, and Karsten Kreis. Align your latents: High-resolution video synthesis with latent diffusion models. In *IEEE Conference on Computer Vision and Pattern Recognition (CVPR)*, 2023. 1
- [3] Xin Chen, Biao Jiang, Wen Liu, Zilong Huang, Bin Fu, Tao Chen, and Gang Yu. Executing your commands via motion diffusion in latent space. In *Proceedings of the IEEE/CVF Conference on Computer Vision and Pattern Recognition*, pages 18000–18010, 2023. 1, 2, 4
- [4] Eli Chien, Chao Pan, and Olgica Milenkovic. Certified graph unlearning. In *NeurIPS 2022 Workshop: New Frontiers in Graph Learning*, 2022. 2
- [5] Jungbin Cho, Junwan Kim, Jisoo Kim, Minseo Kim, Mingyu Kang, Sungeun Hong, Tae-Hyun Oh, and Youngjae Yu. Discord: Discrete tokens to continuous motion via rectified flow decoding, 2024. 2, 5
- [6] Jade Copet, Felix Kreuk, Itai Gat, Tal Remez, David Kant, Gabriel Synnaeve, Yossi Adi, and Alexandre Défossez. Simple and controllable music generation. In *Proceedings of the 37th International Conference on Neural Information Processing Systems*, 2023. 1
- [7] Lucas Dixon, John Li, Jeffrey Sorensen, Nithum Thain, and Lucy Vasserman. Measuring and mitigating unintended bias in text classification. In *Proceedings of the 2018 AAAI/ACM Conference on AI, Ethics, and Society*, 2018. 1
- [8] Chongyu Fan, Jiancheng Liu, Yihua Zhang, Eric Wong, Dennis Wei, and Sijia Liu. Salun: Empowering machine unlearning via gradient-based weight saliency in both image classification and generation. In *The Twelfth International Conference on Learning Representations*, 2024. 2
- [9] Hao Fei, Shengqiong Wu, Wei Ji, Hanwang Zhang, and Tat-Seng Chua. Dysen-vdm: Empowering dynamics-aware text-to-video diffusion with llms. *2024 IEEE/CVF Conference on Computer Vision and Pattern Recognition (CVPR)*, 2023. 1
- [10] Rohit Gandikota, Joanna Materzynska, Jaden Fiotto-Kaufman, and David Bau. Erasing concepts from diffusion models. *2023 IEEE/CVF International Conference on Computer Vision (ICCV)*, pages 2426–2436, 2023. 1
- [11] Rohit Gandikota, Hadas Orgad, Yonatan Belinkov, Joanna Materzyńska, and David Bau. Unified concept editing in diffusion models. In *2024 IEEE/CVF Winter Conference on Applications of Computer Vision (WACV)*, 2024. 1, 2, 4, 5, 6
- [12] Chao Gong, Kai Chen, Zhipeng Wei, Jingjing Chen, and Yu-Gang Jiang. Reliable and efficient concept erasure of text-to-image diffusion models. In *Computer Vision – ECCV 2024: 18th European Conference*, 2024. 1, 2, 4, 5, 6
- [13] Chuan Guo, Tom Goldstein, Awni Y. Hannun, and Laurens van der Maaten. Certified data removal from machine learning models. In *International Conference on Machine Learning*, 2019. 1, 2
- [14] Chuan Guo, Shihao Zou, Xinxin Zuo, Sen Wang, Wei Ji, Xingyu Li, and Li Cheng. Generating diverse and natural 3d human motions from text. In *2022 IEEE/CVF Conference on Computer Vision and Pattern Recognition (CVPR)*, 2022. 1, 3, 6
- [15] Chuan Guo, Yuxuan Mu, Muhammad Gohar Javed, Sen Wang, and Li Cheng. Momask: Generative masked modeling of 3d human motions. In *Proceedings of the IEEE/CVF Conference on Computer Vision and Pattern Recognition*, pages 1900–1910, 2024. 2, 4, 5, 6, 7
- [16] Biao Jiang, Xin Chen, Wen Liu, Jingyi Yu, Gang Yu, and Tao Chen. Motiongpt: Human motion as a foreign language. *arXiv preprint arXiv:2306.14795*, 2023. 1, 2, 4, 5, 7
- [17] Nupur Kumari, Bingliang Zhang, Sheng-Yu Wang, Eli Shechtman, Richard Zhang, and Jun-Yan Zhu. Ablating concepts in text-to-image diffusion models. In *International Conference on Computer Vision (ICCV)*, 2023. 1
- [18] Guihong Li, Hsiang Hsu, Chun-Fu Chen, and Radu Marculescu. Machine unlearning for image-to-image generative models. In *The Twelfth International Conference on Learning Representations*, 2024. 2
- [19] Jing Lin, Ailing Zeng, Shunlin Lu, Yuanhao Cai, Ruimao Zhang, Haoqian Wang, and Lei Zhang. Motion-x: A large-scale 3d expressive whole-body human motion dataset. *Advances in Neural Information Processing Systems*, 2023. 1, 3, 6
- [20] Shilin Lu, Zilan Wang, Leyang Li, Yanzhu Liu, and Adams Wai-Kin Kong. Mace: Mass concept erasure in diffusion models. In *Proceedings of the IEEE/CVF Conference on Computer Vision and Pattern Recognition (CVPR)*, 2024. 1, 2, 5
- [21] Mathis Petrovich, Michael J. Black, and Gül Varol. TEMOS: Generating diverse human motions from textual descriptions. In *European Conference on Computer Vision (ECCV)*, 2022. 2
- [22] Ekkasit Pinyoanuntapong, Muhammad Usama Saleem, Pu Wang, Minwoo Lee, Srijan Das, and Chen Chen. Bamm: Bidirectional autoregressive motion model. In *European Conference on Computer Vision*, 2024. 2, 4, 5, 6, 7
- [23] Dustin Podell, Zion English, Kyle Lacey, Andreas Blattmann, Tim Dockhorn, Jonas Müller, Joe Penna, and Robin Rombach. Sdxl: Improving latent diffusion models for high-resolution image synthesis, 2023. 5
- [24] Alec Radford, Jong Wook Kim, Chris Hallacy, Aditya Ramesh, Gabriel Goh, Sandhini Agarwal, Girish Sastry, Amanda Askell, Pamela Mishkin, Jack Clark, Gretchen Krueger, and Ilya Sutskever. Learning transferable visual models from natural language supervision. *CoRR*, abs/2103.00020, 2021. 5
- [25] Robin Rombach, A. Blattmann, Dominik Lorenz, Patrick Esser, and Björn Ommer. High-resolution image synthesis with latent diffusion models. *2022 IEEE/CVF Conference on Computer Vision and Pattern Recognition (CVPR)*, 2021. 1
- [26] Robin Rombach, Andreas Blattmann, Dominik Lorenz, Patrick Esser, and Björn Ommer. High-resolution image synthesis with latent diffusion models. *CoRR*, abs/2112.10752, 2021. 5

- [27] Nataniel Ruiz, Yuanzhen Li, Varun Jampani, Yael Pritch, Michael Rubinstein, and Kfir Aberman. Dreambooth: Fine tuning text-to-image diffusion models for subject-driven generation. *2023 IEEE/CVF Conference on Computer Vision and Pattern Recognition (CVPR)*, 2022. 1
- [28] Siva Sai, Uday Mittal, Vinay Chamola, Kaizhu Huang, Indro Spinelli, Simone Scardapane, Zhiyuan Tan, and Amir Hussain. Machine un-learning: an overview of techniques, applications, and future directions. *Cognitive Computation*, 2024. 2
- [29] Alessio Sampieri, Alessio Palma, Indro Spinelli, and Fabio Galasso. Length-aware motion synthesis via latent diffusion. In *European Conference on Computer Vision*, 2024. 1, 2, 4, 7
- [30] Agon Serifi, Ruben Grandia, Espen Knoop, Markus Gross, and Moritz Bächer. Robot motion diffusion model: Motion generation for robotic characters. In *SIGGRAPH Asia 2024 Conference Papers*, pages 1–9, 2024. 1
- [31] Alex Tamkin, Mohammad Taufeque, and Noah D. Goodman. Codebook features: Sparse and discrete interpretability for neural networks, 2023. 5
- [32] Guy Tevet, Sigal Raab, Brian Gordon, Yoni Shafir, Daniel Cohen-or, and Amit Haim Bermanto. Human motion diffusion model. In *The Eleventh International Conference on Learning Representations*, 2023. 2
- [33] Andrea Tirinzoni, Ahmed Touati, Jesse Farebrother, Mateusz Guzek, Anssi Kanervisto, Yingchen Xu, Alessandro Lazaric, and Matteo Pirota. Zero-shot whole-body humanoid control via behavioral foundation models. In *NeurIPS 2024 Workshop on Open-World Agents*, 2024. 1
- [34] Aaron van den Oord, Oriol Vinyals, and Koray Kavukcuoglu. Neural discrete representation learning. In *Proceedings of the 31st International Conference on Neural Information Processing Systems (NIPS)*, 2017. 2, 4
- [35] Heng Xu, Tianqing Zhu, Lefeng Zhang, Wanlei Zhou, and Philip S. Yu. Machine unlearning: A survey. *ACM Comput. Surv.*, 2023. 1, 2
- [36] Yue Yang, Yuqi Lin, Hong Liu, Wenqi Shao, Runjian Chen, Hailong Shang, Yu Wang, Yu Qiao, Kaipeng Zhang, and Ping Luo. Position: towards implicit prompt for text-to-image models. In *Proceedings of the 41st International Conference on Machine Learning*, 2024. 3
- [37] Jianrong Zhang, Yangsong Zhang, Xiaodong Cun, Shaoli Huang, Yong Zhang, Hongwei Zhao, Hongtao Lu, and Xi Shen. T2m-gpt: Generating human motion from textual descriptions with discrete representations. In *Proceedings of the IEEE/CVF Conference on Computer Vision and Pattern Recognition (CVPR)*, 2023. 1, 2, 4, 5, 7

# Human Motion Unlearning –Supplementary Material–

Edoardo De Matteis<sup>1\*</sup> Matteo Migliarini<sup>1,2\*</sup> Alessio Sampieri<sup>2</sup> Indro Spinelli<sup>1</sup> Fabio Galasso<sup>1</sup>  
<sup>1</sup>Sapienza University of Rome, Italy <sup>2</sup>ItalAI

This document provides additional details to support the main paper. It includes an in-depth discussion of our alignment training-free machine unlearning approach, a comprehensive comparison of methods, and extra qualitative results. Next, we present the formulas for the evaluation metrics used in our experiments and outline key implementation details. We encourage readers to view the supplementary videos available in the `index.html` file and the provided folder.

## Contents

<a href="#">1. Alignment Training-Free Machine Unlearning</a>	<a href="#">1</a>
<a href="#">2. Comparison</a>	<a href="#">2</a>
<a href="#">3. Extra qualitative results</a>	<a href="#">4</a>
<a href="#">4. Metrics</a>	<a href="#">5</a>
<a href="#">5. Implementation Details</a>	<a href="#">5</a>

## 1. Alignment Training-Free Machine Unlearning

When adapting UCE [2] and RECE [3] for human motion unlearning, it is necessary to predefine the target keyword the toxic motions will be mapped to. We experiment with three different keywords: “walk”, “stand”, and an empty string. Walking and standing are among the most frequent actions in the dataset and often serve foundations for more complex motions. The keyword “stand” appears in various prompts, referring to different nuances of the action, such as “standing still” or “standing up”. Similarly, the keyword “walk” may correspond to different directional variations, like “walking left” or “walking right”. The empty string, on the other hand, provides greater flexibility by allowing the model to remain less constrained by a predefined target, and aligns with the target chosen in [2, 3]. Our results in Table 1 indicate that using the empty string generally leads to better performance. Therefore, we adopt it as the primary choice in the main paper.

	Forget Set				Retain Set				
	FID→	MM-Notox↓	Diversity→	R@1→	FID↓	MM-Nontox↓	Diversity→	R@1↑	
MoMask $\mathcal{D}_r$	8.435±.295	11.254±.064	15.721±.255	0.119±.007	4.508±.103	8.270±.015	19.560±.332	0.332±.002	
MoMask w/ UCE	“Stand”	43.660±.516	6.350±.034	<b>9.173</b> ±.083	<b>0.110</b> ±.004	1.379±.027	3.653±.008	10.178±.113	0.233±.001
	“Walk”	75.764±.823	7.930±.047	6.980±.070	0.090±.004	10.851±.079	4.910±.010	8.698±.108	0.193±.001
	“ ”	<b>25.039</b> ±.442	<b>5.106</b> ±.045	8.693±.067	0.105±.005	<b>0.395</b> ±.008	<b>3.101</b> ±.007	<b>10.194</b> ±.091	<b>0.257</b> ±.001
MoMask w/ RECE	“Stand”	75.091±.957	9.037±.063	<b>8.765</b> ±.107	0.058±.003	<b>5.780</b> ±.029	<b>4.482</b> ±.007	9.518±.137	<b>0.195</b> ±.001
	“Walk”	120.591±.1.092	10.599±.038	4.926±.102	0.039±.002	49.341±.226	8.953±.013	6.339±.117	0.066±.0007
	“ ”	<b>58.487</b> ±.899	<b>8.183</b> ±.047	8.591±.073	<b>0.069</b> ±.004	12.557±.092	6.531±.015	<b>9.612</b> ±.147	0.121±.001

Table 1. Comparison of UCE and RECE across different target concepts, evaluated on HumanML3D.

\*Equal contribution.

## 2. Comparison

We present the complete results for the forget and retain sets on the HumanML3D [4] dataset, evaluating multimodality and R-precision at top-2 and top-3 for both MoMask [5] and BAMB [10]. Then, we report the corresponding results for the Motion-X [7] dataset.

**HumanML3D.** Table 2 presents the expanded results on the forget set of the HumanML3D dataset. LCR consistently outperforms UCE and RECE across all reported metrics for MoMask. While BAMB w/ RECE shows slightly better Diversity and MultiModality scores, LCR achieves a 32.6% improvement on MM-Notox and a 15.8% increase on R@3.

On the retain set, RECE generally achieves better performance on MultiModality, while LCR improves all other metrics across the board.

	Forget Set						
	FID $\rightarrow$	MM-Notox $\downarrow$	Diversity $\rightarrow$	MultiModality $\rightarrow$	R@1 $\rightarrow$	R@2 $\rightarrow$	R@3 $\rightarrow$
MoMask $\mathcal{D}_r$	13.644 $\pm$ .365	4.392 $\pm$ .041	7.611 $\pm$ .088	2.215 $\pm$ .065	0.129 $\pm$ .004	0.234 $\pm$ .005	0.307 $\pm$ .005
MoMask [5]	0.956 $\pm$ .084	5.047 $\pm$ .031	6.146 $\pm$ .092	1.687 $\pm$ .041	0.159 $\pm$ .005	0.284 $\pm$ .008	0.363 $\pm$ .007
MoMask $FT$	6.367 $\pm$ .236	4.723 $\pm$ .038	6.488 $\pm$ .058	2.122 $\pm$ .061	0.145 $\pm$ .006	0.257 $\pm$ .007	0.331 $\pm$ .008
MoMask w/ UCE	25.039 $\pm$ .442	5.106 $\pm$ .045	8.693 $\pm$ .083	2.624 $\pm$ .082	0.105 $\pm$ .004	0.192 $\pm$ .005	0.256 $\pm$ .007
MoMask w/ RECE	58.487 $\pm$ .899	8.183 $\pm$ .047	8.591 $\pm$ .073	4.174 $\pm$ .124	0.069 $\pm$ .003	0.129 $\pm$ .004	0.179 $\pm$ .005
MoMask w/ LCR	<b>12.434</b> $\pm$ .303	<b>4.723</b> $\pm$ .035	<b>6.580</b> $\pm$ .066	<b>2.441</b> $\pm$ .065	<b>0.133</b> $\pm$ .004	<b>0.240</b> $\pm$ .006	<b>0.307</b> $\pm$ .004
BAMB $\mathcal{D}_r$	15.604 $\pm$ .334	4.552 $\pm$ .041	7.688 $\pm$ .074	3.343 $\pm$ .073	0.122 $\pm$ .005	0.219 $\pm$ .004	0.284 $\pm$ .007
BAMB [10]	1.353 $\pm$ .107	4.911 $\pm$ .053	6.202 $\pm$ .089	1.994 $\pm$ .003	0.164 $\pm$ .007	0.286 $\pm$ .008	0.370 $\pm$ .010
BAMB $FT$	1.443 $\pm$ .118	4.914 $\pm$ .050	6.224 $\pm$ .098	2.028 $\pm$ .048	0.161 $\pm$ .006	0.284 $\pm$ .007	0.368 $\pm$ .008
BAMB w/ UCE	57.953 $\pm$ .893	7.809 $\pm$ .068	9.482 $\pm$ .073	7.863 $\pm$ .178	0.074 $\pm$ .003	0.137 $\pm$ .005	0.182 $\pm$ .005
BAMB w/ RECE	34.367 $\pm$ .484	6.796 $\pm$ .048	<b>7.740</b> $\pm$ .073	<b>3.680</b> $\pm$ .076	0.061 $\pm$ .004	0.111 $\pm$ .006	0.158 $\pm$ .005
BAMB w/ LCR	<b>9.712</b> $\pm$ .214	<b>4.597</b> $\pm$ .033	6.502 $\pm$ .077	2.569 $\pm$ .050	<b>0.136</b> $\pm$ .005	<b>0.247</b> $\pm$ .007	<b>0.316</b> $\pm$ .005

Table 2. Forget set full comparison on HumanML3D.

	Retain Set						
	FID $\downarrow$	MM-Notox $\downarrow$	Diversity $\rightarrow$	MultiModality $\uparrow$	R@1 $\uparrow$	R@2 $\uparrow$	R@3 $\uparrow$
MoMask $\mathcal{D}_r$	0.093 $\pm$ .003	2.700 $\pm$ .007	10.059 $\pm$ .080	2.713 $\pm$ .007	0.291 $\pm$ .001	0.511 $\pm$ .002	0.668 $\pm$ .002
MoMask [5]	0.064 $\pm$ .002	2.714 $\pm$ .005	10.143 $\pm$ .081	1.824 $\pm$ .029	0.290 $\pm$ .001	0.509 $\pm$ .001	0.669 $\pm$ .001
MoMask $FT$	0.088 $\pm$ .002	2.803 $\pm$ .007	10.143 $\pm$ .097	1.546 $\pm$ .026	0.280 $\pm$ .001	0.514 $\pm$ .002	0.672 $\pm$ .002
MoMask w/ UCE	0.395 $\pm$ .008	3.101 $\pm$ .007	10.194 $\pm$ .091	1.829 $\pm$ .039	0.257 $\pm$ .001	0.459 $\pm$ .002	0.610 $\pm$ .002
MoMask w/ RECE	12.557 $\pm$ .092	6.531 $\pm$ .015	9.612 $\pm$ .147	<b>3.493</b> $\pm$ .076	0.121 $\pm$ .001	0.221 $\pm$ .001	0.301 $\pm$ .001
MoMask w/ LCR	<b>0.077</b> $\pm$ .002	<b>2.720</b> $\pm$ .005	<b>10.106</b> $\pm$ .086	1.855 $\pm$ .033	<b>0.287</b> $\pm$ .001	<b>0.504</b> $\pm$ .001	<b>0.665</b> $\pm$ .001
BAMB $\mathcal{D}_r$	0.566 $\pm$ .015	3.123 $\pm$ .009	10.092 $\pm$ .093	2.335 $\pm$ .062	0.279 $\pm$ .001	0.484 $\pm$ .002	0.634 $\pm$ .002
BAMB [10]	0.135 $\pm$ .004	2.698 $\pm$ .009	10.118 $\pm$ .100	1.714 $\pm$ .035	0.302 $\pm$ .001	0.522 $\pm$ .001	0.678 $\pm$ .002
BAMB $FT$	0.163 $\pm$ .005	2.731 $\pm$ .007	10.109 $\pm$ .086	1.773 $\pm$ .045	0.301 $\pm$ .002	0.519 $\pm$ .001	0.673 $\pm$ .002
BAMB w/ UCE	4.296 $\pm$ .063	5.119 $\pm$ .014	9.654 $\pm$ .080	<b>4.699</b> $\pm$ .113	0.184 $\pm$ .001	0.327 $\pm$ .002	0.435 $\pm$ .002
BAMB w/ RECE	13.310 $\pm$ .118	7.062 $\pm$ .015	8.470 $\pm$ .094	4.003 $\pm$ .039	0.122 $\pm$ .001	0.216 $\pm$ .022	0.291 $\pm$ .002
BAMB w/ LCR	<b>0.140</b> $\pm$ .005	<b>2.699</b> $\pm$ .008	<b>10.068</b> $\pm$ .102	1.732 $\pm$ .038	<b>0.299</b> $\pm$ .001	<b>0.519</b> $\pm$ .001	<b>0.675</b> $\pm$ .002

Table 3. Retain set full comparison HumanML3D.

**Motion-X.** Motion-X appears particularly challenging for BAMB [10].

The FID of our re-trained BAMB is in line with the values reported by their original paper for the HumanML3D dataset. Also, the FID of our retrained MoMask on Motion-X is in line with the values reported by their original paper, just expectedly slightly larger due to the more challenging and noise nature of Motion-X.

The performance of the re-trained BAMB on Motion-X yields a very large FID of 54.451. Since our other re-trainings appear valid, we feel confident of the reported FID value. We believe that, beyond re-training, Motion-X appears to require specific setups which we cannot find documented in the open-source BAMB code. We leave these numbers out of the main paper, as courtesy to authors, and because we believe that better due diligence may be attempted in collaboration with authors, at the earliest authors’ availability.

Although notably larger, the figures for LCR applied to BAMB on Motion-X are in line with all previous results and demonstrate that LCR consistently outperforms the other selected baselines. In the forget set (Table 4), our model achieves the best MM-Notox score, outperforming the second-best technique by 9.1% with MoMask and 13.38% with BAMB. Additionally, BAMB w/ LCR achieves the best performance on retrieval metrics.

In the retain set (Table 5), LCR improves FID by 28.9% and 38.7% when applied to MoMask and BAMB, respectively. UCE achieves the best MM-Notox score, while LCR performs best on Diversity and R@3, with a 7.5% improvement.

	Forget Set						
	FID →	MM-Notox ↓	Diversity →	MultiModality →	R@1 →	R@2 →	R@3 →
MoMask $\mathcal{D}_r$	8.435±.295	11.254±.064	15.721±.255	5.052±.172	0.119±.007	0.209±.006	0.288±.006
MoMask [5]	2.028±.127	9.001±.071	15.884±.219	4.327±.153	0.289±.008	0.420±.009	0.515±.005
MoMask $FT$	2.072±.099	9.085±.050	15.855±.050	4.344±.156	0.280±.007	0.413±.008	0.506±.009
MoMask w/ UCE	<b>10.522</b> ±.223	10.931±.028	6.648±.112	2.563±.090	<b>0.033</b> ±.001	<b>0.059</b> ±.004	<b>0.087</b> ±.005
MoMask w/ RECE	12.704±.327	12.422±.034	6.241±.132	2.836±.102	0.031±.003	<b>0.059</b> ±.004	<b>0.087</b> ±.005
MoMask w/ LCR	2.218±.159	<b>9.930</b> ±.092	<b>15.606</b> ±.210	<b>4.623</b> ±.173	0.283±.007	0.414±.008	0.508±.006
BAMB $\mathcal{D}_r$	59.585±1.552	15.913±.087	11.352±.228	7.985±.165	0.084±.004	0.148±.006	0.205±.007
BAMB [10]	56.215±1.799	14.982±.131	11.441±.218	7.877±.165	0.119±.005	0.198±.009	0.261±.009
BAMB $FT$	54.723±2.140	14.798±.114	11.497±.262	7.968±.151	0.122±.006	0.197±.007	0.261±.008
BAMB w/ UCE	67.165±1.614	17.469±.099	11.801±.307	8.397±.170	0.051±.004	0.095±.005	0.138±.005
BAMB w/ RECE	67.468±1.383	17.800±.077	8.967±.340	6.759±.146	0.019±.002	0.038±.004	0.055±.006
BAMB w/ LCR	<b>53.639</b> ±1.933	<b>15.132</b> ±.122	<b>11.402</b> ±.257	<b>7.927</b> ±.170	<b>0.112</b> ±.005	<b>0.192</b> ±.007	<b>0.252</b> ±.007

Table 4. Forget set full comparison on Motion-X.

	Retain Set						
	FID ↓	MM-Notox ↓	Diversity →	MultiModality ↑	R@1 ↑	R@2 ↑	R@3 ↑
MoMask $\mathcal{D}_r$	4.508±.103	8.270±.015	19.560±.332	5.198 ±.150	0.332±.002	0.484±.002	0.585±.002
MoMask [5]	2.686±.045	8.076±.017	19.366±.214	5.447±.167	0.344±.001	0.503±.002	0.606±.002
MoMask $FT$	3.325±.060	8.070±.019	19.405±.228	5.506±.176	0.347±.002	0.508±.003	0.607±.002
MoMask w/ UCE	3.740±.041	<b>6.863</b> ±.008	6.243±.059	2.398±.073	0.046±.001	<b>0.508</b> ±.003	<b>0.607</b> ±.002
MoMask w/ RECE	14.287±.133	7.351±.013	6.342±.062	2.901±.094	0.029±.001	0.058±.001	0.088±.001
MoMask w/ LCR	<b>2.656</b> ±.043	8.261±.019	<b>19.260</b> ±.216	<b>5.535</b> ±.179	<b>0.335</b> ±.001	0.490±.002	0.593±.002
BAMB $\mathcal{D}_r$	41.739±.457	13.918±.030	13.689±.163	7.875±.161	0.144±.002	0.238±.003	0.311±.003
BAMB [10]	54.451±.588	14.526±.033	12.944±.166	8.010±.172	0.135±.002	0.224±.002	0.293±.002
BAMB $FT$	54.746±.760	14.545±.045	12.900±.186	7.905±.179	0.136±.002	0.225±.002	0.294±.002
BAMB w/ UCE	88.951±.753	<b>11.314</b> ±.160	16.646±.036	<b>8.297</b> ±.155	0.087±.001	0.154±.002	0.210±.002
BAMB w/ RECE	137.043±.311	18.293±.021	7.966±.132	6.770±.131	0.026±.001	0.053±.001	0.083±.002
BAMB w/ LCR	<b>54.481</b> ±.523	14.631±.032	<b>12.839</b> ±.186	8.057±.170	<b>0.132</b> ±.001	<b>0.217</b> ±.002	<b>0.285</b> ±.002

Table 5. Retain set full comparison on Motion-X.

### 3. Extra qualitative results

**Implicit motion.** Human actions can be described in different ways without explicitly using a word that has been flagged as toxic. For instance, instead of saying “*throwing a kick*”, a malicious user of a T2M model could phrase it as “*a man swings his right leg back and forth*”. A naive filtering mechanism could easily be tricked by avoiding banned words. Since unlearning aims to forget concepts, it is fundamental that an unlearning mechanism is robust against such type of circumvention attempts. Figure 1 illustrates this specific scenario, it can be seen how LCR appears to effectively withstand this type of attacks, even when unlearning based on UCE fails.

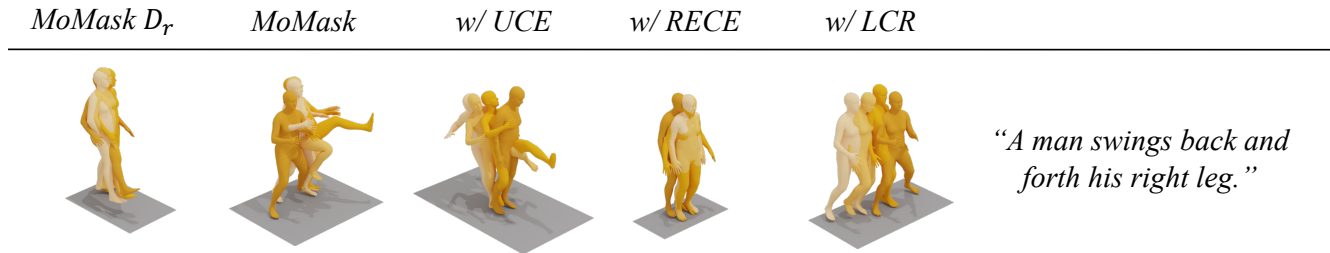


Figure 1. Example of implicit motion de-toxified.

**Causal Intervention.** Our LCR approach is based on the intuition that codes in a discrete space are disentangled, and can represent specific actions. For this reason, we perform unlearning by replacing codes associated with toxicity. To further support this, we show toxicity injection on human motion. First, we identify codes associated to a toxic motion, like kicking. Then, given a safe prompt, we inject toxic codes in the latent sequence  $Z$ . In Figure 2 we show that toxicity injection: we can see that even though the given prompts are safe, adding specific codes allows the model to perform kicks. Specifically, code 140 represents a high kick with the left leg, while code 344 represents a lower kick with the right leg.

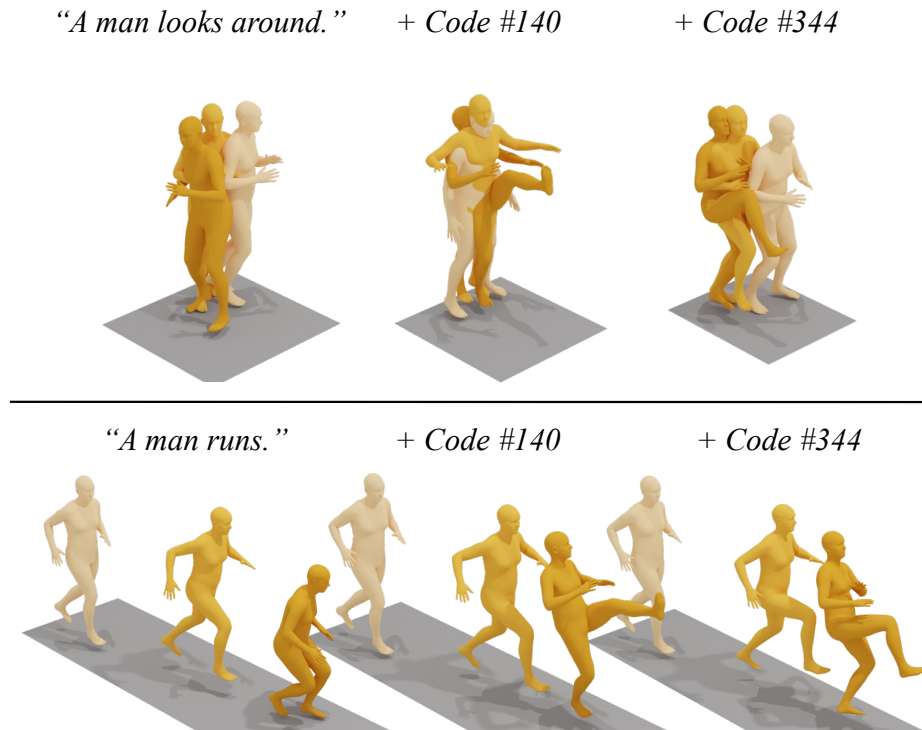


Figure 2. Examples of causal intervention.

## 4. Metrics

We provide the mathematical formulations for evaluating the generated results based on established literature [1, 4–6, 10–13].

**R-Precision and MM-Notox.** In text-to-motion tasks, [4] introduces motion and text feature extractors that produce geometrically aligned representations for paired text-motion samples. Within this feature space, we compute R-Precision by embedding generated motions alongside mismatched samples and measuring the top-1/2/3 retrieval accuracy. Additionally, we assess Multi-modal Notox Distance (MM-Notox), which quantifies the discrepancy between generated motions and their corresponding de-toxified text descriptions. Both R-Precision and MM-Notox are computed using L2-loss.

**FID.** Motion quality is evaluated using the Fréchet Inception Distance (FID), which compares the statistical similarity between the distributions of generated and real motions. This is achieved by computing the L2-loss between their latent feature representations.

**Diversity and MultiModality.** Diversity and MultiModality metrics are employed to measure both the overall variability in generated motions and the diversity of motions corresponding to the same text prompt.

Diversity is computed by randomly splitting the generated motion set into two equal-sized subsets,  $\{m_1, \dots, m_{\mathcal{M}_d}\}$  and  $\{m'_1, \dots, m'_{\mathcal{M}_d}\}$ , each containing motion feature vectors. It is then defined as:

$$\text{Diversity} = \frac{1}{\mathcal{M}_d} \sum_{i=1}^{\mathcal{M}_d} \|m_i - m'_i\|. \quad (1)$$

MultiModality is assessed by first selecting  $T_d$  random text descriptions from the dataset. For each text description, we sample two equal-sized subsets of motion feature vectors, denoted as  $\{m_{t,1}, \dots, m_{t,\mathcal{M}_d}\}$  and  $\{m'_{t,1}, \dots, m'_{t,\mathcal{M}_d}\}$ . Multi-Modality is then computed as:

$$\text{MultiModality} = \frac{1}{T_d \cdot \mathcal{M}_d} \sum_{t=1}^{T_d} \sum_{i=1}^{\mathcal{M}_d} \|m_{t,i} - m'_{t,i}\|. \quad (2)$$

## 5. Implementation Details

**UCE and RECE.** The algorithms from UCE [2] and RECE [3] have been readapted for human motion unlearning. Originally, these methods operated on the cross-attention mechanism between text and motion embeddings. However, since the T2M models MoMask [5] and BAMB [10] do not incorporate cross-attention, we instead apply the method to the projection embedding that maps the CLIP embedding to the motion embedding.

**Motion-X.** Motion-X [7] provides SMPL-X [9] motion data, which includes detailed hand and facial features. To align this dataset with our setup, we first process it using the official code provided by its authors<sup>1</sup> to convert SMPL-X motion features into SMPL [8] representations.

Next, to ensure consistency with HumanML3D [4], we preprocess the text prompts using the Semantic Role Labeling (SRL) tool provided by the HumanML3D authors<sup>2</sup>. Some manual refinements are applied due to variations in the formatting of prompts within the Motion-X dataset.

Additionally, since Motion-X is organized as multiple datasets, we restructure it into a format that closely resembles HumanML3D by flattening its structure. We will release this newly processed dataset to the community, appropriately crediting the original authors.

For evaluation purposes, the feature extraction has been trained following [4]’s implementation<sup>3</sup>, for 300 epochs.

---

<sup>1</sup><https://github.com/IDEA-Research/Motion-X>

<sup>2</sup><https://github.com/EricGuo5513/HumanML3D>

<sup>3</sup><https://github.com/EricGuo5513/text-to-motion>

**Training.** We train MoMask and BAMB on Motion-X and on the clean  $\mathcal{D}_r$  splits of HumanML3D and Motion-X. We run up to 50 epochs for the VQ-VAE and up to 500 epochs for the Masked and Residual Transformers, stopping training once the loss plateaus.

For MoMask, we train the entire pipeline, composed by the VQ-VAE, the masked transformer, and residual transformer. For BAMB, which builds upon MoMask by modifying only the masked transformer, we do not retrain the residual transformer, as this is also restricted by the original code implementation. Our training is conducted on a single NVIDIA A100 GPU. On Motion-X, training all stages of MoMask takes approximately 34 hours. Training from scratch on the cleaned versions of HumanML3D and Motion-X takes approximately one day for each dataset.

When finetuning our models, we do it for five additional epochs, requiring about 10 minutes in total for both the masked and residual transformers. Our LCR method takes approximately 15 seconds.

## References

- [1] Xin Chen, Biao Jiang, Wen Liu, Zilong Huang, Bin Fu, Tao Chen, and Gang Yu. Executing your commands via motion diffusion in latent space. In *Proceedings of the IEEE/CVF Conference on Computer Vision and Pattern Recognition*, pages 18000–18010, 2023. 5
- [2] Rohit Gandikota, Hadas Orgad, Yonatan Belinkov, Joanna Materzyńska, and David Bau. Unified concept editing in diffusion models. In *2024 IEEE/CVF Winter Conference on Applications of Computer Vision (WACV)*, 2024. 1, 5
- [3] Chao Gong, Kai Chen, Zhipeng Wei, Jingjing Chen, and Yu-Gang Jiang. Reliable and efficient concept erasure of text-to-image diffusion models. In *Computer Vision – ECCV 2024: 18th European Conference*, 2024. 1, 5
- [4] Chuan Guo, Shihao Zou, Xinxin Zuo, Sen Wang, Wei Ji, Xingyu Li, and Li Cheng. Generating diverse and natural 3d human motions from text. In *2022 IEEE/CVF Conference on Computer Vision and Pattern Recognition (CVPR)*, 2022. 2, 5
- [5] Chuan Guo, Yuxuan Mu, Muhammad Gohar Javed, Sen Wang, and Li Cheng. Momask: Generative masked modeling of 3d human motions. In *Proceedings of the IEEE/CVF Conference on Computer Vision and Pattern Recognition*, pages 1900–1910, 2024. 2, 3, 5
- [6] Biao Jiang, Xin Chen, Wen Liu, Jingyi Yu, Gang Yu, and Tao Chen. Motiongpt: Human motion as a foreign language. *arXiv preprint arXiv:2306.14795*, 2023. 5
- [7] Jing Lin, Ailing Zeng, Shunlin Lu, Yuanhao Cai, Ruimao Zhang, Haoqian Wang, and Lei Zhang. Motion-x: A large-scale 3d expressive whole-body human motion dataset. *Advances in Neural Information Processing Systems*, 2023. 2, 5
- [8] Matthew Loper, Naureen Mahmood, Javier Romero, Gerard Pons-Moll, and Michael J. Black. SMPL: A skinned multi-person linear model. *ACM Trans. Graphics (Proc. SIGGRAPH Asia)*, 34(6):248:1–248:16, 2015. 5
- [9] Georgios Pavlakos, Vasileios Choutas, Nima Ghorbani, Timo Bolkart, Ahmed A. A. Osman, Dimitrios Tzionas, and Michael J. Black. Expressive body capture: 3D hands, face, and body from a single image. In *Proceedings IEEE Conf. on Computer Vision and Pattern Recognition (CVPR)*, pages 10975–10985, 2019. 5
- [10] Ekkasit Pinyoanuntapong, Muhammad Usama Saleem, Pu Wang, Minwoo Lee, Srijan Das, and Chen Chen. Bamm: Bidirectional autoregressive motion model. In *European Conference on Computer Vision*, 2024. 2, 3, 5
- [11] Alessio Sampieri, Alessio Palma, Indro Spinelli, and Fabio Galasso. Length-aware motion synthesis via latent diffusion. In *European Conference on Computer Vision*, 2024.
- [12] Guy Tevet, Sigal Raab, Brian Gordon, Yoni Shafir, Daniel Cohen-or, and Amit Haim Bermano. Human motion diffusion model. In *The Eleventh International Conference on Learning Representations*, 2023.
- [13] Jianrong Zhang, Yangsong Zhang, Xiaodong Cun, Shaoli Huang, Yong Zhang, Hongwei Zhao, Hongtao Lu, and Xi Shen. T2m-gpt: Generating human motion from textual descriptions with discrete representations. In *Proceedings of the IEEE/CVF Conference on Computer Vision and Pattern Recognition (CVPR)*, 2023. 5